Geotech Geol Eng (2010) 28:851–864
DOI 10.1007/s10706-010-9348-y

ORIGINAL PAPER

Soil Permeability Controlled by Particle–Fluid Interaction

Marcos A. Montoro · Franco M. Francisca

Received: 16 February 2009 / Accepted: 19 July 2010 / Published online: 29 July 2010

Abstract In this paper, Atterberg limits and hydraulic conductivity tests are performed in sand samples mixed with different amounts of silt, zeolite and bentonite. The testing liquids consist of kerosene, two paraffin oils with different viscosities, distilled water and 1, 10 and 1,000 mol/m^3 calcium chloride solutions. Experimental results show that soils completely lost their plasticity when are in contact with light non-aqueous phase liquids, and that the liquid limit depends on the dynamic viscosity of the fluid surrounding the particles. Also, tested soils show different hydraulic conductivity with water before and after Ca^{2+} ions are introduced in the permeating fluid, in agreement with the change in the formation Gibbs free energy and diffuse double layer theory. Finally, the influence of viscosity ratio, specific surface of particles, soil fabric and PFI on hydraulic conductivity is discussed and related to the effective particle diameter and soil void ratio.

Electronic supplementary material The online version of this article (doi:10.1007/s10706-010-9348-y) contains supplementary material, which is available to authorized users.

M. A. Montoro · F. M. Francisca
Consejo de Investigaciones Científicas y Técnicas (CONICET), Córdoba, Argentina

M. A. Montoro · F. M. Francisca (✉)
Departamento de Construcciones Civiles, Universidad Nacional de Córdoba, Av. Velez Sarsfield 1611, 5016 Córdoba, Argentina
e-mail: ffrancis@efn.uncor.edu

Keywords Double layer · Soil pollution · Flow · Light non-aqueous phase liquid (LNAPL) · Liquid limit · Permeability and hydraulic conductivity · Soil fabric

1 Introduction

The main forces that control the displacement of fluids in the pores of coarse soils depend on gravity, viscosity and capillarity (Mercer and Cohen 1990). Interfacial forces only take place when soil pores contain immiscible fluids (e.g. water and oil, air and water) and dictate the movement of menisci during imbibition and drainage phenomena (Hardisty et al. 1998). In absence of interfaces, the driving force and losses during fluid displacement are related to the hydraulic gradient and viscous effect, respectively. Consequently, the hydraulic conductivity of soils is controlled by both soil and pore fluid properties. Due to that, there are several accepted formulations to evaluate the soil hydraulic conductivity (k) in terms of grain and index properties (Vuković and Soro 1992). Recently, Lee et al. (2005) observe that the liquid limit, sedimentation volume and swell index show a critical threshold in the increase of k, and Sridharan and Nagaraj (2005) obtain accurate predictions in terms of the void ratio and shrinkage index. Respect to the fluid properties, there is clear evidence that hydraulic conductivity increases when the ionic concentration or valence raises in the

permeating fluid (Jo et al. 2001; Lee et al. 2005). However, most of empirical, statistical and phenomenological models to predict the hydraulic conductivity of soils ignore the effect of particle–fluid interaction (Dullien 1992).

The presence of fine particles influences the hydro-mechanical properties of soils since particle–fluid interaction (PFI) becomes relevant in high specific surface materials (Schmitz 2006). PFI is relevant only in the case of fine soils or coarse soils with silt and clay contents as high as 7% (Santamarina et al. 2001). In this case, the chemical properties of the pore fluid and electrical forces govern the interaction between phases and determine particle association and flocculation (van Olphen 1977; Mitchell and Soga 2005). This soil micro-structure is then determined by the factors controlling the attraction and repulsion forces between particles, which can be understand from the double layer and van der Waals effects (Israelachvili 1992).

Several geoenvironmental engineering phenomena are influenced by this electrostatic interaction between phases, usually, when soils are contaminated with organic and inorganic fluids (Sharma and Reddy 2004). This liquid–mineral interaction affects several geotechnical properties of soils including Atterberg limits, soil fabric and correlated properties (permeability, strength, etc. Kaya and Fang 2005; Khamehchiyan et al. 2007).

Atterberg limits provide a useful tool to evaluate the effect of PFI on soil behavior since liquid limit (LL) and plastic index (IP) can be related to soil mineralogy (e.g. Seed et al. 1964; Schmitz et al. 2004) and to the pore fluid chemistry (Acar et al. 1985; Gleason et al. 1997; Candelaria and Matsumoto 2000).

The chemical properties of the fluid affect ion hydration and the formation of the diffuse double layer around soil particles. Hence, fluid chemistry directly affects the soil fabric and the hydraulic properties of the porous media (Mitchell and Soga 2005). This PFI becomes relevant for the design of liners and slurry walls, soil remediation, reactive flow and mass transport mechanisms (Fetter 1993; Ruhl and Daniel 1997).

The purpose of this article is to evaluate the influence of PFI on the displacement of organic and inorganic liquids in soils. Atterberg limits and permeability are related to the viscosity of immiscible organic liquids in contact with soil particles. The simultaneous effect of the ionic concentration in the fluid phase and the fine particle content in the soil allows evaluating the importance of PFI on the hydraulic properties of porous media. Finally, fabric changes are inferred from the evolution of soil intrinsic permeability with the different chemical properties of the permeating fluids.

2 Background

2.1 Particle–Fluid Interaction

PFI phenomenon arises due to the electrical surface charge of soil particles and the physical–chemical properties of the liquid (e.g. presence of ions, polarizability, etc.). Water molecules near the mineral surface are affected by the electric field of the particle since water is a polar molecule (dipole moment $= 6.2 \times 10^{-30}$ Cm). Then, water molecules near the particles rotate and align the hydrogen atoms to the mineral surface. In case of electrolytes, the water molecules hydrate cations and anions attracted by their electric fields. In this case, the electric field generated by the particles attracts and repulses the hydrated cations and anions, respectively (Mitchell and Soga 2005). This process modifies the water physical properties at short distances from the mineral surface.

Two different liquid layers, separated by the outer Helmholtz plane, are identified at short distances from the mineral surface. The first is known as Stern layer and holds cations and water molecules with low mobility and strongly attracted to the mineral surface. The second is the Gouy diffuse layer and contains water molecules and hydrated ions influenced by the surface electric potential, which decreases with the ion concentration (Israelachvili 1992).

The electric potential (ψ_x) decreases exponentially with the distance from the mineral surface. In the case of symmetrical 1:1 electrolytes (e.g. NaCl), the initial value is equal to the surface electric potential (ψ_0) and the final one reduces to zero at infinite distance. Assuming a low surface potential, the rate of change is given by the Debye-Hückel equation (Santamarina et al. 2001):

$$\psi_x \approx \psi_0 \, e^{-x/\vartheta} \tag{1}$$

The characteristic decay length of the potential, ϑ (m), is known as Debye-Hückel length, or "double

layer thickness", and is related to the liquid properties as follows:

$$\vartheta = \sqrt{\frac{\varepsilon_0 R\,\kappa' T}{2F^2 c_0 z^2}} \tag{2}$$

where $R = 8.314$ J/(K mol) is the universal gas constant, $F = 9.6485 \times 10^4$ C/mol is the Faraday's constant, $\varepsilon_0 = 8.85 \times 10^{-12}$ F/m is the vacuum dielectric permittivity, $T =$ temperature (K), $c_0 =$ bulk electrolyte concentration (mol/m^3), $\kappa' =$ real relative permittivity, and $z =$ ionic valence. If the pore fluid is water ($\kappa' = 78.5$) and $T = 293$ K, Eq. (2) reduces to (Israelachvili 1992):

$$\vartheta = \frac{C}{\sqrt{c_0}} \times 10^{-12} \tag{3}$$

where C is a constant related to the ion valence, $C = 9.61$ for 1:1 electrolytes, $C = 5.57$ for 1:2 and 2:1 electrolytes (e.g. $CaCl_2$) and $C = 4.8$ for 2:2 electrolytes (e.g. $MgSO_4$).

The counterions in the double layer can be replaced by other hydrated cations while electroneutrality is preserved. The valence and size of the cation control the replaceability, even the surface charge density, thermal agitation and ionic concentration are also important. This cation movement in and out of double layer, or adsorption–desorption reactions, can be expressed by means of the following stoichiometric relationship (Adamson and Gast 1997):

$$\mathrm{AR} + \mathrm{B} \leftrightarrow \mathrm{BR} + \mathrm{A} \tag{4}$$

where R represent the mineral surface, A is an adsorbed counterion which is completely replaced by other counterion B. This reaction is only possible when the change of Gibbs free energy, ΔG, is negative:

$$\Delta G = \Delta h - T\Delta S \tag{5}$$

where $h =$ enthalpy, $T =$ absolute temperature and $S =$ entropy. The negative value of ΔG indicates that entropy tends to increase. The spontaneity of this reaction can only be changed by adding energy to the system (Sposito 2008).

In the case of organic contaminants-filled porosity, the real relative permittivity becomes relevant for the surface potential and double layer thickness (Mitchell and Soga 2005). Alcohols, oil, solvents and other non-aqueous phase liquids (NAPL) have very low permittivity in comparison with that of water or electrolytes (CRC 2008). In contact with clay particles, the double layers are shorter than in the case of water. Then, if water or an electrolyte is replaced by an organic fluid inside the soil pores, the double layer thickness reduces. Eventually, this phenomenon can macroscopically emerge as volumetric contractions and cracks (Gleason et al. 1997; Jo et al. 2001; Kolstad et al. 2004).

Double layers of two adjacent particles interact with each other generating particle repulsion. At the same time, attractive van der Waals forces cause attraction between colloidal particles. The balance between repulsive double layer and attractive van der Waals forces gives the net force known as DLVO that governs the fabric formation in soils (Palomino and Santamarina 2005). Repulsive and attractive net forces produce dispersed and flocculated soil fabrics, respectively. Among other soil and fluid properties, the fabric is of fundamental importance for the hydraulic conductivity of soils (Mitchell et al. 1965; Benson and Trast 1995; Kaya and Fang 2005; Schmitz 2006).

2.2 Hydraulic Conductivity and Intrinsic Permeability

Soil hydraulic conductivity, k (m/s), depends on porous media and liquid properties. Conversely, absolute or intrinsic permeability, K (m^2), is independent of these variables and is assumed as a porous media property by geotechnical engineers and soil scientists. The Kozeny-Carman equation presents a theoretical relationship between k, K and relevant soil and fluid properties as follow (Mitchell and Soga 2005):

$$K = k\left(\frac{\mu}{\rho g}\right) = \frac{1}{k_0\,T^2\,S_0^2}\left(\frac{e^3}{1+e}\right)S^3 \tag{6}$$

where $g =$ gravity, $\rho =$ fluid density and $\mu =$ fluid viscosity, $T =$ tortuosity, $k_0 =$ pore shape factor, $S_0 =$ wetted surface area per unit volume of particles, $e =$ void ratio and $S =$ degree of saturation.

The relationship between k and the ionic valence or concentration is related to the effect of these two fluid properties on the double layer thickness (Eq. 2). When the double layer shrinks, soil fabric tends to a more flocculated state and there is more space

available for fluid flow giving an increase of hydraulic conductivity. The pre-hydration of clay particles with electrolytes has important effects on fabric formation. Soils with high specific surface initially saturated with electrolytes and deionized-water show high and low hydraulic conductivities respectively, when permeated with the same chemical solution (Gleason et al. 1997; Ruhl and Daniel 1997).

Ruhl and Daniel (1997) and Jo et al. (2001) state that hydraulic conductivity of bentonite decreases up to three orders of magnitude when the pH of the solution changes from 2 to 14. This behavior is attributed to the higher negative surface charge of clay particles in contact with high pH solutions (Greberg and Kjellander 1998). In this case, the double layer thickness is large and clay particles are dispersed due to electrostatic repulsion (Palomino and Santamarina 2005).

When the permeating liquid is an organic fluid, the hydraulic conductivity is affected either by the real relative permittivity κ' in the case of polar molecules (e.g. ethyl alcohol) since the double layer thickness tends to decrease according to Eq. (2), or due to the impossibility to form a double layer in the case of non-aqueous phase liquids (NAPLs) (e.g. carbon tetrachloride). Experimental evidence shows that the presence of organic fluids increases the hydraulic conductivity of fine soils (Gnanapragasam et al. 1995). Kaya and Fang (2005) demonstrate that kaolinite and bentonite particles tend to form flocculated structures when they are in contact with organic fluids. In addition, Schmitz (2006) shows that the affect of changing the double layer thickness on k should be considered simultaneously with the effective confining pressure.

Finally, intrinsic permeability (K) considers the physical properties of the fluid phase, but ignores its chemical nature and phase interaction mechanisms. Then, any variation of K observed when a permeating fluid is substituted by another having different chemical properties suggests that soil fabric fluctuates (Aringhieri and Giachetti 2001). When PFI and double layer effects are negligible (e.g. in case of NAPL as permeating fluid), K becomes a unique soil property and the kinematic viscosity of each permeating fluid ($\upsilon = \mu/\rho$) is responsible for the observed changes in hydraulic conductivity (Fetter 1993):

$$k_j = k_i \frac{\upsilon_i}{\upsilon_j} \tag{7}$$

Jarsjö et al. (1997) report a very good agreement between the predicted values from Eq. (7) and measured hydraulic conductivities of several soil samples (from sands to peats) tested with kerosene of different kinematic viscosities. The differences between computed and measured values reported by these authors are lower than 18% in all cases.

3 Materials and Methods

3.1 Soils and Fluids

The soils used in this study are sand, silt, zeolite and bentonite (Trademark "Minarmco"). A qualitative optic diffraction test reveals that the sand is mainly composed by pure minerals including silica (43%), feldspars (12%) and muscovite (1%) and rock fractions composed by granite (38%) and other clasts in a less percentage. The silt is mainly composed by quartz, feldspar, volcanic glass and igneous rocks fragments (typical volumetric content of each fraction is reported by Teruggi 1957). X-ray diffraction tests show that the natural zeolite is a mix of clinoptilolite and heulandite. The bentonite has more than 92% of sodium montmorillonite (data provided by manufacturer). Table 1 shows the most relevant physical properties, and Online Resource 1 presents SEM pictures showing the dominant particle shape of these soils.

The organic fluids used are three LNAPLs including kerosene and two paraffin oils with different viscosity. The inorganic fluids used are distilled water and 1, 10 and 1000 mol/m^3 of $CaCl_2$ solutions. The main physicochemical properties of these fluids are summarized in Table 2.

3.2 Atterberg Limits

The liquid limit of the fine-grained soils (silt, zeolite and bentonite) was performed by using all the fluids presented in Table 2 and following the recommendations of the ASTM D4318 standard procedure (ASTM 2007).

Table 1 Main physical properties of tested soils

Property	Sand	Silt	Zeolite	Bentonite	Standard
Specific Gravity	2.68	2.63	2.49	2.67	ASTM D 854[b]
D_{50} (mm)	1	0.05	0.011	N/A	ASTM D 422[b]
D_{10} (mm)	0.41	0.0008	0.0001	N/A	ASTM D 422[b]
Particles < 0.074 mm (%)	1.28	61.4	100	100	ASTM D 422[b]
Particles < 0.002 mm (%)	0	20.88	32.76	84.77	ASTM D 422[b]
Coefficient of uniformity	2.93	87.50	200	N/A	ASTM D 422[b]
Coefficient of curvature	0.94	1.45	1.62	N/A	ASTM D 422[b]
Specific surface, Ss (m^2/gr)	0.001–0.04[a]	0.04–1.1[a]	61.2	731	Santamarina et al. (2002)
CEC (mEq/100gr)	1.27×10^{-4}–0.005	0.005–0.14	7.82	93.4	Santamarina et al. (2002)
USCS	SP	CL–ML	MH	CH	ASTM D 2487[b]

NP no plastic, *N/A* not available, *CEC* cation exchange capacity

[a] Santamarina et al. (2001), [b] ASTM (2007)

Table 2 Main physical properties of tested fluid

Property	Kerosene	Paraffin Oil V90	Paraffin Oil V180	Water	$CaCl_2$ 1 mol/m^3	$CaCl_2$ 10 mol/m^3	$CaCl_2$ 1000 mol/m^3
Density (kg/m^3)	830	846	867	1,000	1,000	1,000	1000.1
Viscosity (Ns/m^2)	2.05×10^{-3}	0.015	0.03	1.01×10^{-3}	1.01×10^{-3}	1.01×10^{-3}	1.10×10^{-3}
Real permittivity (50 MHz)	~2	~2	~2	78.5	80	90.8	N/A
Electric conductivity (S/m)	$<10^{-4}$	$<10^{-4}$	$<10^{-4}$	1.26×10^{-3}	3.13×10^{-2}	0.227	18.94
pH	–	–	–	5	5.5	5.5	6
Water solubility	Insoluble	Insoluble	Insoluble	–	–	–	–
Color	Red	Colorless	Colorless	Colorless	Colorless	Colorless	Colorless
Odor	Strong	Odorless	Odorless	Odorless	Odorless	Odorless	Odorless

3.3 Sample Preparation and Hydraulic Conductivity Tests

Soil specimens were oven dried at 105°C during 24 h and after that several samples were prepared by mixing the sand fraction with 2, 5, 12 and 25% by weight of silt, zeolite or bentonite. These specimens were mixed with either water or the organic fluids (Table 2) and compacted in the testing cell in three layers of equal height by giving 25 blows per layer with a 10.95 mm in diameter blunt tip bar (specimens tested with the $CaCl_2$ solutions were compacted with destilled water). The compaction moisture content was 10% in all cases except for the sand mixed with 12 and 25% of bentonite were the liquid content was higher than the bentonite liquid limit in order to ensure homogeneity. Table 3 presents the attained initial void ratios. In most of cases, the samples compacted with organic fluids have smaller void ratios than that compacted with water even the compaction method remains constant. These results indicate that coordination number and soils particle arrangement are determined by the compacting fluid and possible PFI mechanisms. Finally, the cells were connected to a burette and three pore volumes of flow were flushed through the specimen before starting the permeability tests.

The number of hydraulic conductivity measurements performed in this work includes 62 tests. (39 with organic fluids, 13 with distilled water, and 10 compacted with distilled water and permeated with the $CaCl_2$ electrolytes). The hydraulic conductivity

Table 3 Initial void ratios of tested samples

Soil	Fine content (%)	Void ratio				
		Water	Kerosene	Paraffin oil V90	Paraffin oil V180	$CaCl_2$ electrolyte[a]
Sand	0	0.79	0.67	0.56	0.55	0.66
Sand + silt	2	0.71	0.58	0.55	0.58	–
	5	0.74	0.56	0.51	0.50	0.5
	12	0.80	0.49	0.44	0.42	0.31
	25	0.72	0.44	0.41	0.35	0.31
Sand + zeolite	2	0.56	0.60	0.53	0.53	–
	5	0.56	0.55	0.52	0.52	0.49
	12	0.58	0.43	0.37	0.42	0.45
	25	0.66	0.61	0.63	0.47	0.74
Sand + bentonite	2	0.83	0.60	0.49	0.50	–
	5	0.89	0.58	0.51	0.48	0.20
	12	0.58	0.46	0.43	0.38	0.84
	25	1.08	0.44	0.44	0.47	1.16

[a] One specimen is tested with different concentrations (0, 1, 10 and 1,000 mol/m^3)

was measured in rigid wall permeameters by means of the falling head technique and following the ASTM D5856 standard procedure (ASTM 2007). The hydraulic gradients ranged from 4 to 35 for high and low permeability samples, respectively. The rigid wall permeameter was selected instead of flexible wall permeameters because the tests performed herein were comparatively similar to chemical compatibility tests (volumetric shrinkage and crack formation are allowed but swelling is constrained).

The hydraulic conductivity was measured at least three times, or until three consecutive lectures differ no more than ±30%, and an average of these lectures were reported as the test result. The time of testing vary between 7 and 120 days for the highest and lowest permeable sample, respectively.

All hydraulic conductivity measurements were made in the same sample when the permeating fluids were $CaCl_2$ solutions. The $CaCl_2$ concentration was increased from 0 to 1, 10 and 1,000 mol/m^3. Finally, after testing the sample with the highest concentration, the permeating fluid was changed by distilled water. The hydraulic conductivity and electric conductivity of the fluid recovered in the outlet port were measured every pore volume of flow. The conductivity measurements were performed with an Altromix CT2™ meter. The concentration was changed when the recovered fluid attained constant conductivity or when any of the termination criteria given in the ASTM D6766 standard was reached (ASTM 2007).

4 Results and Discussion

4.1 Influence of PFI on Atterberg Limits

Table 4 shows the liquid limits, LL, and plastic index, PI, measured for the silt, zeolite and bentonite tested with water, kerosene, paraffin oils and $CaCl_2$ solutions. Both LL and PI tends to decrease when the soils are in contact with the $CaCl_2$ solutions. An apparent anomalous behavior is observed for the concentration of 1 mol/m^3, attributed here to the intrinsic variability of this test and that the concentration is lower than the minimum electrolyte concentration necessary to produce flocculation or fabric changes (van Olphen 1977; Lee et al. 2005). In

Table 4 Atterberg limits of soils determined with different fluids

Fluid	Silt		Zeolite		Bentonite	
	LL	PI	LL	PI	LL	PI
Water	25.3	8.0	49.9	7.8	301.0	231.0
$CaCl_2$ 1 mol/m^3	24.5	8.1	53.8	7.4	321.8	277.4
$CaCl_2$ 10 mol/m^3	22.2	6.1	51.8	6.0	263.5	218.5
$CaCl_2$ 1,000 mol/m^3	20.9	4.5	47.5	4.8	103.7	63.4
Kerosene	24.5	–	35.8	–	33.5	–
Paraffin oil V90	15.9	–	27.3	–	22.2	–
Paraffin oil V180	11.0	–	10.4	–	12.3	–

LL liquid limit, *PI* plastic index

contact with the non-polar organic liquids, soils behave as non-plastic and show liquid limits lower than that measured with water.

Figure 1a shows the variation of the liquid limits of silt, zeolite and bentonite with the dynamic viscosity of the fluid inside the pores. Experimental results show that LL decreases as the fluid viscosity increases. This trend is attributed here to the multi-phase nature of soils (e.g. solid particles and liquids). Fluid viscosity is a measure of shear resistance of liquids, according to the fluid mechanics, while liquid limit is an indirect measure of the undrained shear strength of normally consolidated soils (Holtz and Kovacs 1981; Santamarina et al. 2001). Then, the decrease of LL shown in Fig. 1a can be associated with a higher expected undrained shear strength of the tested samples produced by the physical properties of the fluid inside the pores. In addition, computed DLVO forces show that the net force is attractive, which favors flocculated fabric to occur and is consistent with an increase in the undrained shear strength (Seed et al. 1960).

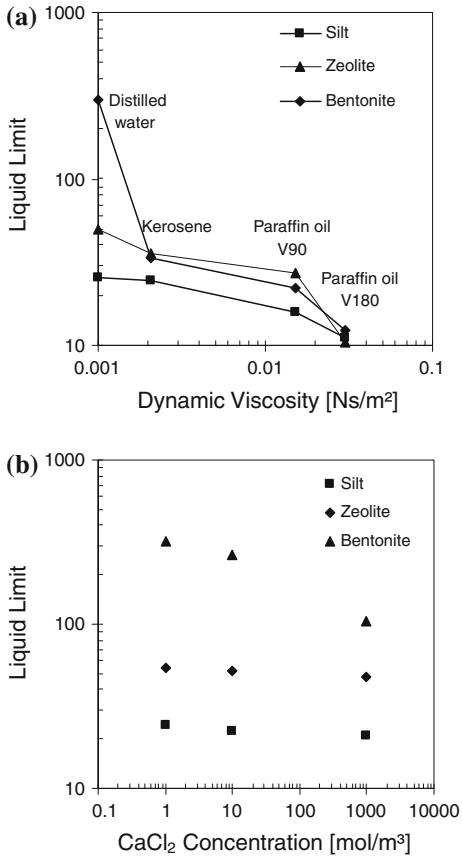

Fig. 1 **a** Influence of the dynamic viscosity of fluids on liquid limit, **b** influence of $CaCl_2$ concentration on liquid limit

Figure 1b presents the influence of $CaCl_2$ concentration on the LL of silt, zeolite and bentonite. There is a clear linear decrease of LL with the ionic concentration, which can be attributed to the lower expected DDL thickness as stated in Eq. (2). This effect depends on the soil specific surface and on the ratio between the DDL and particle thicknesses, resulting in significant changes in the case of bentonite in comparison with that observed in the silt and zeolite specimens. Similar trends are reported by Gleason et al. (1997) for Na- and Ca-montmorillonite in contact with NaCl and $CaCl_2$ electrolytes. Obtained results show the usefulness of Atterberg limits to evaluate PFI effects on soil behavior.

4.2 Influence of Fluid Properties on Permeability

Figure 2 shows the measured intrinsic permeability of sand samples with different contents of silt, zeolite and bentonite. The permeating fluids are distilled water and electrolytes with 10 and 1,000 mol/m^3 of $CaCl_2$. The sand specimens permeated with distilled water, Fig. 2a, show a clear dependence on the fine content and on the specific surface. Fine particle contents above than 5% induces permeability changes as high as four orders of magnitude depending on soil mineralogy, or specific surface. Similar trends are observed when the distilled water is replaced by calcium chloride solutions (Fig. 2b, c). The sand specimens mixed with silt show almost no influence of the fluid change on the measured permeabilities. Conversely, permeability rises when the fine particles are zeolite and bentonite.

The relative importance of permeability changes observed when the ion concentration increases is determined by the related decrease of the DDL thickness (Eq. 3). Two different mechanisms are responsible of this macro-scale observation. On one hand, the bentonite contains expandable minerals (weak interlayer bonding) and most of water is forming the DDL around particles. In this case, any change of K can be associated to expansion/shrinkage mechanisms in response to changes in the DDL thickness. On the other hand, in the case of zeolite and silt, most of water is free within the pore space even the DDL is present. In this type of soil the

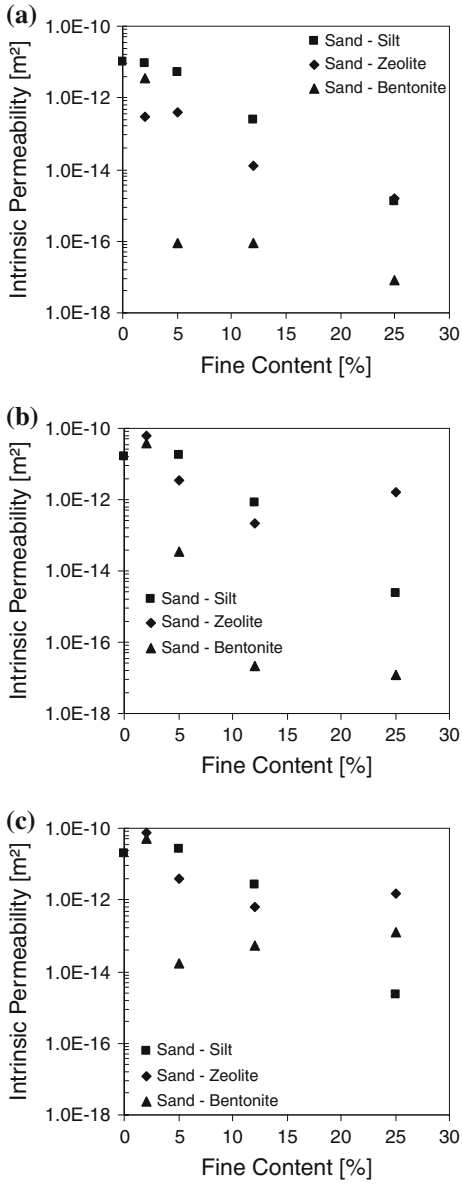

Fig. 2 Effect of fine particle content and $CaCl_2$ concentration on soil intrinsic permeability. **a** Distilled water, **b** $CaCl_2$ 10 mol/m^3, **c** $CaCl_2$ 1,000 mol/m^3

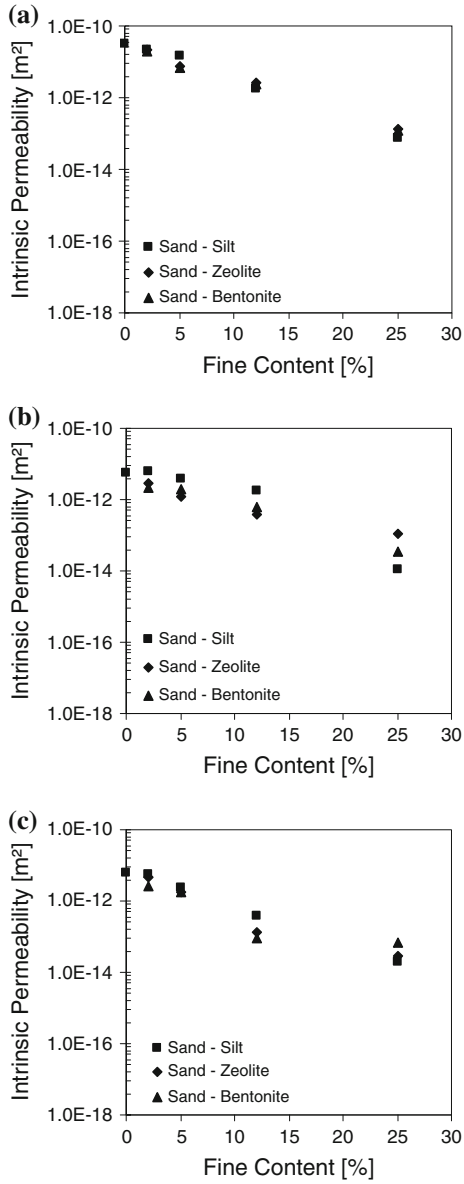

Fig. 3 Influence of fine particle content on the intrinsic permeability of sand–silt, sand–zeolite and sand–bentonite mixtures permeated with organic fluids. **a** Kerosene, **b** paraffin oil V90, **c** paraffin oil V180

observed changes in K can be associated to differences in the pore space available to flow due to variations in the DDL thickness (and the amount of water that can freely move inside the pores).

Then, the relevance of chemical interactions on K can be associated to the specific surface and presence of expansive minerals in soils. In addition, the changes in K highlight the effect of PFI on the fabric of porous media in coincidence with the more flocculated state expected at higher ion concentrations. This evolution of soil fabric emerges at macroscale as the observed increase of intrinsic permeability shown in Fig. 2b, c.

Figure 3 presents the influence of silt, zeolite and bentonite on the permeability of sand samples permeated with kerosene, paraffin oil V90 and paraffin oil V180. In this case, there is a clear effect

of fine particle content but a very slight influence of fine type. The reductions of K take place within a range of only two orders of magnitude; while for similar specimens permeated with distilled water and electrolytes this effect produces changes of up to six orders of magnitude (Fig. 2).

The relative low relevance of PFI mechanisms observed in the specimens permeated with non-polar organic fluids is responsible of the narrow range of permeability observed at each fine particle contents. The small dispersion observed in the data is attributed to the different initial soil void ratio (Table 3). Neither kerosene, nor paraffin oil can develop a diffuse double layer around the soil particles. Then, there is a higher effective space within the pores available for fluid displacement when the specimens are permeated with LNAPLs than with water or electrolytes. As a result, K measured with LNAPLs is always higher than that determined with distilled water and inorganic fluids.

Figure 4 shows the evolution of hydraulic and electrical conductivities with the number of pore volumes of flow for the sand (Fig. 4a) and sand with 25% of zeolite (Fig. 4b) specimens. The associated time of permeation is also indicated in the figure. The sand specimen displays no changes of hydraulic conductivity while the electrical conductivity of the fluid recovered in the outlet port varies according to the chemical properties of the permeating fluid. However, electrical and hydraulic conductivities present similar changes for the sand specimen containing 25% of zeolite. There are clear increases/decreases of hydraulic conductivity associated with the increases/decreases of electrical conductivity. This behavior is attributed to the influence of ion concentration on the double layer thickness (Eq. 3) and to the effect of micro-fabric on the hydraulic conductivity (Mitchell and Soga 2005).

A very interesting phenomenon is observed when the concentration is decreased by replacing the 1,000 mol/m^3 of $CaCl_2$ solution with distilled water. This change produces a clear decrease in the electrical conductivity of the recovered fluid. The hydraulic conductivity follows this reduction, but never reaches the initial values registered before to introducing the $CaCl_2$ into the sample. Figure 5 presents the influence of the electrical conductivity of the recovered fluid on the measured hydraulic conductivity for the

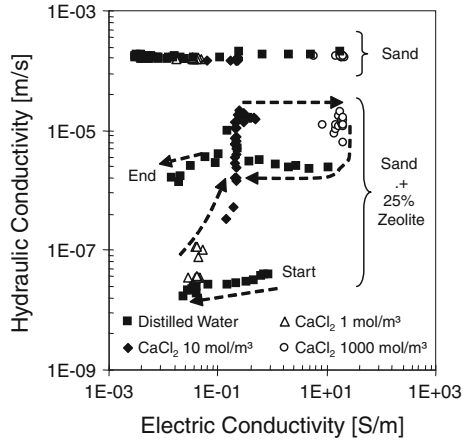

Fig. 5 Influence of the electrical conductivity of the recovered fluid on the hydraulic conductivity of the sand and sand + 25% zeolite

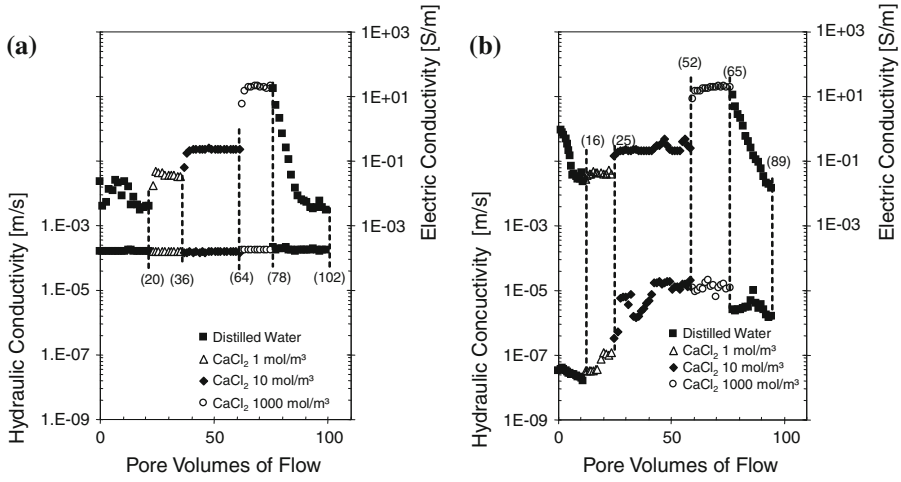

Fig. 4 Soil hydraulic conductivity and fluid electrical conductivity with the number of pore volumes of flow and the successive changes of $CaCl_2$ concentration. **a** Sand, **b** Sand + 25% zeolite. Time of permeation in days is indicated between brackets

sand and sand with 25% of zeolite specimens. The hydraulic conductivity of sand presents negligible variations with the electrical conductivity confirming the insignificant effect of PFI on the permeability of coarse-grained soils. In the case of sand with zeolite, the observed behavior shows a loop-like shape but the final hydraulic conductivity differs of the initial one, even for the same electrical conductivity of the permeating fluid.

Soils containing fine particles show similar behavior to that shown in Figs. 4 and 5. Even the initial and final permeating fluids are the same; the final hydraulic conductivity of the specimen is higher than the original. This trend is attributed to the different thicknesses of double layers expected in each case, since when the concentration of the pore fluid decreases the removal of adsorbed Ca^{2+} ions requires additional energy. The Gibbs free energy (Eq. 5) can be used to explain these adsorption-desorption reactions (Adamson and Gast 1997; Sposito 2008). The chemical reaction for the adsorption of Ca^{2+} ions on the mineral surface is as follows:

$$\mathrm{CaCl_2(aq)} + \mathrm{R_2(s)} = \chi\mathrm{CaR_2(s)} + (1-\chi)\mathrm{CaCl_2(aq)} + (1-\chi)\mathrm{R_2(s)} + \chi\mathrm{H_2O} \quad (8)$$

where χ = efficiency factor, R = solid surface available for the reaction, aq = aqueous and s = solid. The change of formation Gibbs free energy (ΔG^0) is computed from the formation free energy (G^0) of each component considering that: (a) $G^0(\mathrm{CaCl_2}) = -553.5$ kJ/mol, (b) $G^0(\mathrm{H_2O}) = -237.19$ kJ/mol, (c) $G^0(\mathrm{CaR_2}) = -31{,}954$ kJ/mol, (d) $G^0(\mathrm{R_2}) = -15{,}698$ kJ/mol (Sposito 2008). Then, the change of formation Gibss free energy ΔG^0 (KJ/mol) becomes:

$$\sum_{\text{products}} G^0 - \sum_{\text{reactants}} G^0 = -242.4\chi \quad (9)$$

The negative sign in the right side of Eq. (9) indicates that the adsorption reaction is possible and spontaneous. Conversely, the change of formation Gibbs free energy for the desorption of Ca^{2+} ions from a mineral surface results 242.4 χ (KJ/mol), which means that the reaction is not possible unless energy is added to the system. This result suggests that Ca^{2+} ions are not completely removed from the media when the chemical composition of the permeating fluids changes from 1,000 mol/m^3 $CaCl_2$ solution to distilled water. Consequently, the thickness of the diffuse double layer is lower than that predicted by Eq. (3) and the final hydraulic conductivity with water remains higher than that measured prior to the permeation with the $CaCl_2$ solutions. The determined influence of mineralogy and fluid chemistry on permeability is very important when the soils are considered as construction materials for permeable barriers or liners.

Several theoretical and empirical models relate permeability with a characteristic grain size or the finer fraction of a particulate medium (e.g. Hazen's empirical equation—Holtz and Kovacs 1981; Dullien 1992; Santamarina et al. 2001). Figure 6 shows the influence of the effective particle diameter (D_{10}) on the intrinsic permeability of sand–silt (a), sand–zeolite (b) and sand–bentonite (c) mixtures. In the case of sand–silt mixtures (low specific surface materials), permeability results display a nearly linear relationship regardless the chemistry of the permeating fluid, with a scattering lower than 2 orders of magnitude. The dispersion of permeability for any effective particle diameter increases as the specific surface of the fine fraction increases, as in the case of zeolite (Fig. 6b) and bentonite (Fig. 6c). In the case of sand-bentonite mixtures the spreading of results increases up to 6 orders of magnitude. The influence of PFI mechanisms on soil fabric and permeability of the fine fraction is responsible of this observed behavior.

From Kozeny-Carman's formula (Eq. 6), permeability has a linear relationship with a function of the void ratio ($e^3/(1+e)$). Figure 7 displays the influence of this void ratio function on the intrinsic permeability of sand mixed with silt, zeolite and bentonite and permeated with the non-polar liquids. Obtained permeabilities show a fairly well linear dependence with the theoretical void ratio function revealed in the Kozeny-Carman's equation. However, extremely high dispersions were obtained when the specimens are permeated with either water or $CaCl_2$ solutions. These results confirm that Kozeny-Carman's formula well predicts soil permeabilities when PFI processes are of low significance.

4.3 Simultaneous Effect of Relative Viscosity and PFI on Hydraulic Conductivity

When the intrinsic permeability (K) can be considered as a distinctive property of the porous media, the

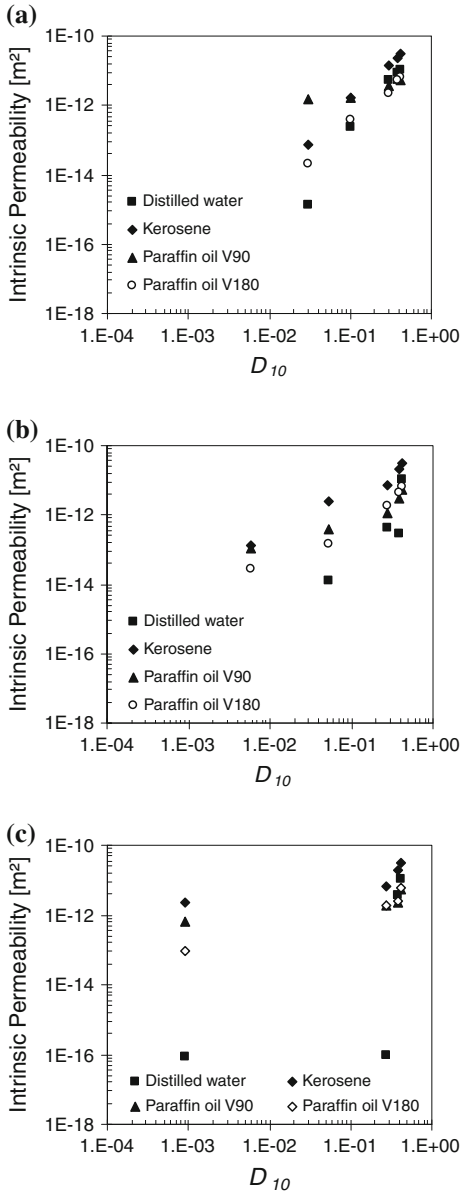

Fig. 6 Influence of the effective grain size (D_{10}) on the intrinsic permeability measured with distilled water and organic fluids. **a** Sand–silt mixtures, **b** sand–zeolite mixtures, **c** sand–bentonite mixtures

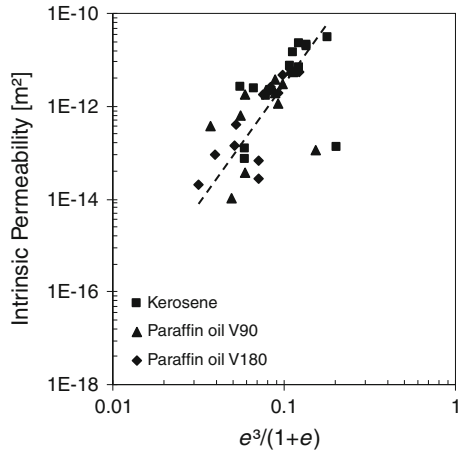

Fig. 7 Effect of Kozeny–Carman void ratio function on the intrinsic permeability measured with organic fluids. Tested samples: sand–silt, sand–zeolite and sand–bentonite mixtures

hydraulic conductivity (k) respect to a given fluid can be predicted from experimental results obtained with a different liquid by means of Eq. (7). In all cases, the limiting factor is the relevance of PFI mechanisms.

Figure 8 shows hydraulic conductivities computed from Eq. (7) as a function of the hydraulic conductivity measured with distilled water. Figure 8a–c show the results obtained for the sand–silt, sand–zeolite and sand–bentonite, respectively. For each soil, the values measured with water overlap the 45° solid line (measured versus predicted hydraulic conductivities). The two dashed lines represent limits of ±1 order of magnitude which can be considered as boundaries of acceptable predictions in the geotechnical field (Benson 1993; Duncan 2000). Only the values computed for the sand–silt mixtures shows deviations lowers than one order of magnitude (Fig. 8a) and the dispersion of data increases significantly in the case of zeolite (Fig. 8b) and bentonite (Fig. 8c). The higher specific surface of bentonite (Ss = 731 m^2/g) and zeolite (Ss = 61.2 m^2/g) respect to the silt (Ss = 0.04–1.1 m^2/g) is responsible of this observed trend. This is related to a relative amount of water inside the DDL higher than the free water inside the pores as the Ss and forces of hydration increases (for the same DDL thickness—Mitchell and Soga 2005). Then, the relative importance of PFI mechanisms in high specific surface materials justify these results and constrain the use of Eq. (7).

Figure 9 presents hydraulic conductivities computed from Eq. (7) as a function of the hydraulic conductivity of sand–silt, sand–zeolite and sand–bentonite measured with kerosene. Hence, the data that overlap the 45° solid line corresponds to values measured with this liquid. In this case, only the values predicted for distilled water are outside the ±1 order of magnitude zone. However, regardless the

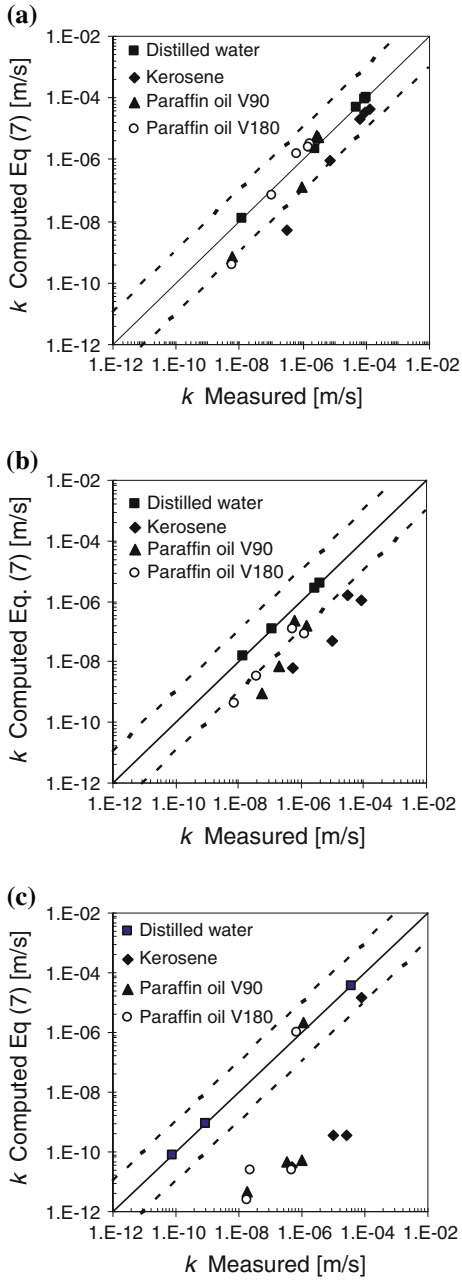

Fig. 8 Comparison between the hydraulic conductivities measured and that computed from Eq. (7) using the measurements with water. **a** Sand–silt, **b** sand–zeolite, **c** sand–bentonite. *Dashed lines* represent a deviation of ±1 order of magnitude

type of soil, almost all predicted values for the two paraffin oils fall within the mean ±1 order of magnitude range. Since PFI mechanisms have almost negligible significance in this case, the obtained

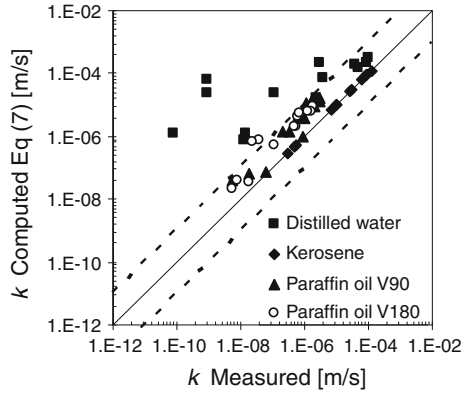

Fig. 9 Comparison between the hydraulic conductivities measured and that computed from Eq. (7) using the measurements with kerosene. Tested samples: sand–silt, sand–zeolite and sand–bentonite mixtures

results show that hydraulic conductivities of soils respect to LNAPLs can be predicted from Eq. (7) using the conductivity measured with another non-polar fluid.

5 Conclusions

This work presents experimental results of Atterberg limits and hydraulic conductivity of sand–silt, sand–zeolite and sand–bentonite mixtures. Different soil samples are tested with selected organic and inorganic liquids in order to evaluate the influence of fluid chemistry, soil fabric, specific surface and fine particle content on relevant soil properties. The main conclusions of this work can be summarized as follows:

- The soil liquid limit reduces when the dynamic viscosity of the liquid surrounding the particles increases. The viscosity of the fluid phase, an indirect measure of fluid shear resistance, affects the liquid limit which is an indirect measure of the undrained shear strength of normally consolidated soils. The presence of ions reduces the liquid limit and soil plasticity. In the case of expandable minerals this phenomenon also induces changes on the thickness of double layer around particles. Then, Atterberg limits can be considered as useful indicators of the importance of PFI phenomena.
- Soils samples with the same amount of fine particles of different specific surface show not

important differences in the intrinsic permeability determined with different LNAPLs. However, the amount of fines, specific surface and fluid chemistry becomes extremely important when the permeating fluid is water or electrolytes.

- The hydraulic conductivity of sand mixed with different contents and type of fine particles depends on the ion concentration in the permeating liquid. Experimental results show that the increase of conductivity is directly related to the rise of both $CaCl_2$ concentration and soil specific surface. In addition, the fluid chemical properties influence both hydraulic conductivity and intrinsic permeability which means that soil fabric changes during permeation.
- The effect of changing the ion concentration in the permeating fluid on double layer and soil permeability is not fully reversible. Counterions can completely adsorb to the mineral surface when the Ca^{2+} concentration rises; and this reaction is spontaneous according to the change of Gibbs free energy. However, when the Ca^{2+} concentrations in the permeating fluid decreases, desorption reaction cannot take place without introducing additional energy to the system. Because of this, the increase of diffuse double layer thickness is lower than the expected thickness and the hydraulic conductivity with distilled water remains higher than that determined before the addition and permeation with the $CaCl_2$ solution.
- The intrinsic permeability can be related to the effective particle diameter (D_{10}) only when PFI mechanisms are of low relevance as in the case of low specific surface materials. When the specific surface is high (e.g. in the case of sand-bentonite mixtures) the fluid properties induce high dispersion in the permeability-D_{10} relationship.
- Intrinsic permeabilities of sand–silt, sand–zeolite and sand–bentonite measured with LNAPLs display a reasonable linear dependence with the theoretical void ratio function of the Kozeny-Carman's equation. However, extremely high dispersion is expected when PFI and soil fabric govern the fluid displacement inside the soil pores.
- The intrinsic permeability can be considered as a soil property when PFI is of low significance, as in the case of nonpolar permeating fluids. In these cases, the soil hydraulic conductivity respect to LNAPLs can be predicted from the relative viscosity and the conductivity measured with a different nonpolar fluid (Eq. 7).

Acknowledgments This research was partially supported by the National Agency for the Promotion of Science and Technology (ANPCyT, research project number PICT2006-822) and the SECyT-UNC (research project number 05/M118). Authors thank the very useful reviewers' comments and M.A.M. thanks the support given by CONICET during this research.

References

Acar YB, Olivieri I, Field SD (1985) Transport of organic contaminants and geotechnical properties of fine—grained soils. Proceedings of the eleventh international conference on soil mechanics and foundation engineering, vol 3, pp 1237–1240

Adamson AW, Gast AP (1997) Physical chemistry of surfaces. Wiley, New York

Aringhieri R, Giachetti M (2001) Effect of sodium adsorption ratio and electrolyte concentrations on the saturated hydraulic conductivity of clay–sand mixtures. Eur J Soil Sci 52(3):449–458. doi:10.1046/j.1365-2389.2001.00404.x

ASTM (2007) Annual book of ASTM Standards, Vol. 04.08. ASTM International, West Conshohocken, PA

Benson CH (1993) Probability distributions for hydraulic conductivity of compacted soil liners. J Geotech Eng 119(3): 471–486. doi:10.1061/(ASCE)0733-9410(1993)119:3(471)

Benson CH, Trast JM (1995) Hydraulic conductivity of thirteen compacted clays. Clays Clay Minerals 43(6):669–681

Candelaria LM, Matsumoto MR (2000) Effects of NAPL contaminants on the permeability of a soil–bentonite slurry wall material. Transp Porous Med 38(1–2):43–56. doi: 10.1023/A:1006655015509

CRC (2008) Handbook of chemistry and physics. In: David R. Lide (ed) 88th edn. Boca Ratón

Dullien FAL (1992) Porous media: fluid transport and porous structure. Academic Press, San Diego

Duncan J (2000) Factor of safety and reliability in geotechnical engineering. J Geotech Geoenviron Eng 126(4):307–316

Fetter CW (1993) Contaminant hydrogeology. Prentice Hall, Upper Saddle River

Gleason MH, Daniel DE, Eykholt GR (1997) Calcium and sodium bentonite for hydraulic containment applications. J Geotech Geoenviron Eng 123(5):438–445

Gnanapragasam N, Lewis BG, Finno R (1995) Microstructural changes in sand–bentonite soils when exposed to aniline. J Geotech Eng 121(2):119–125. doi:10.1061/(ASCE)0733-9410(1995)121:2(119)

Greberg H, Kjellander R (1998) Charge inversion in electric double layers and effect of different sizes for counterions and coions. J Chem Phys 108(7):2940–2953. doi:10.1063/1.475681

Hardisty PE, Wheater HS, Johnston PM, Bracken RA (1998) Behavior of light immiscible liquid contaminants in fractured aquifers. Geotechnique 48(6):747–760

Holtz RD, Kovacs WD (1981) An introduction to geotechnical engineering. Prentice Hall, New Jersey

Israelachvili J (1992) Intermolecular and surface forces. Academic Press, San Diego

Jarsjö J, Destouni G, Yaron B (1997) On the relation between viscosity and hydraulic conductivity for volatile organic liquid mixtures in soils. J Contam Hydrol 25(1–2):113–127. doi:10.1016/S0169-7722(96)00036-8

Jo HY, Katsumi T, Benson CH, Edil TB (2001) Hydraulic conductivity and swelling of nonprehydrated GCLs permeated with single–species salt solutions. J Geotech Geoenviron Eng 127(7):557–567

Kaya A, Fang H (2005) Experimental evidence of reduction in attractive and repulsive forces between clay particles permeated with organic liquids. Can Geotech J 42(2): 632–640. doi:10.1139/t04-099

Khamehchiyan M, Charkhabi AM, Tajik M (2007) Effect of crude oil contamination on geotechnical properties of clayey and sandy soils. Eng Geol 89(3–4):220–229. doi:10.1016/j.enggeo.2006.10.009

Kolstad DC, Benson CH, Edil TB (2004) Hydraulic conductivity and swell of nonprehydrated geosynthetic clay liners permeated with multispecies inorganic solutions. J Geotech Geoenviron Eng 130(12):1236–1249

Lee JM, Shackelford CD, Benson CH, Jo HY, Edil TB (2005) Correlating index properties and hydraulic conductivity of geosynthetic clay liners. J Geotech Geoenviron Eng 131(11): 1319–1329

Mercer JW, Cohen RM (1990) A review of immiscible fluids in the subsurface: properties, models, characterization and remediation. J Contam Hydrol 6(2):107–162. doi:10.1016/0169-7722(90)90043-G

Mitchell JK, Soga K (2005) Fundamentals of soil behavior. Wiley, New York

Mitchell JK, Hooper DR, Campanella RG (1965) Permeability of compacted clay. J Soil Mech Found Div 91(4):41–65

Palomino A, Santamarina JC (2005) Fabric map for kaolinite: effects of pH and ionic concentration on behavior. Clays Clay Minerals 53(3):211–223. doi:10.1346/CCMN.2005.0530302

Ruhl JL, Daniel DE (1997) Geosynthetic clay liners permeated with chemical solutions and leachates. J Geotech Geoenviron Eng 123(4):369–381

Santamarina JC, Klein KA, Fam MA (2001) Soils and waves. Wiley, England

Santamarina JC, Klein KA, Wang YH, Prencke E (2002) Specific surface: determination and relevance. Can Geotech J 39(1):233–241. doi:10.1139/t01-077

Schmitz RM (2006) Can the diffuse double layer theory describe changes in hydraulic conductivity of compacted clay. Geotech Geol Eng 24(6):1835–1844. doi:10.1007/s10706-005-3365-2

Schmitz RM, Schroeder C, Charlier R (2004) Chemo–mechanical interactions in clay: a correlation between clay mineralogy and Atterberg limits. Appl Clay Sci 26(1–4):351–358. doi:10.1016/j.clay.2003.12.015

Seed HB, Mitchell JK, Chan CK (1960) The strength of compacted cohesive soils. Conference on shear strength of cohesive soils, ASCE. University of Colorado, Denver, pp 877–964

Seed HB, Woodward RJ, Lundgren R (1964) Clay mineralogical aspects of the Atterberg limits. J Soil Mech Found Div 90:107–131

Sharma HD, Reddy KR (2004) Geoenvironmental engineering. Wiley, New Jersey

Sposito G (2008) The chemistry of soils. Oxford University Press, London

Sridharan A, Nagaraj HB (2005) Hydraulic conductivity of remolded fine grained soils versus index properties. Geotech Geol Eng 23(1):43–60. doi:10.1007/s10706-003-5396-x

Teruggi ME (1957) The nature and origin of Argentinean loess. J Sed Res 27(3):322–332

van Olphen H (1977) An introduction to clay colloid chemistry: for clay technologists, geologists and soil scientists. Interscience, New York

Vuković M, Soro A (1992) Determination of hydraulic conductivity of porous media from grain size distribution. Water Resources Publications, Littleton